SUPPORTING INFORMATION

A Modular Telechelic Catechol Platform for Tunable Fe- and V-Coordinated Dynamic Polymer Gels

Ferley Orozco,[a] Amy Hammett,[a] Mahshad Karimi,[a] Thomas E. Ericson,[a] Lahiru Pasikku Hannadige,[a] Joshua R. Fabian Jr.,[a] Carol Korzeniewski,[a] Anthony F. Cozzolino,[a] Samantha L. Kristufek[a]*

TABLE OF FIGURES

Synthesis of monomers

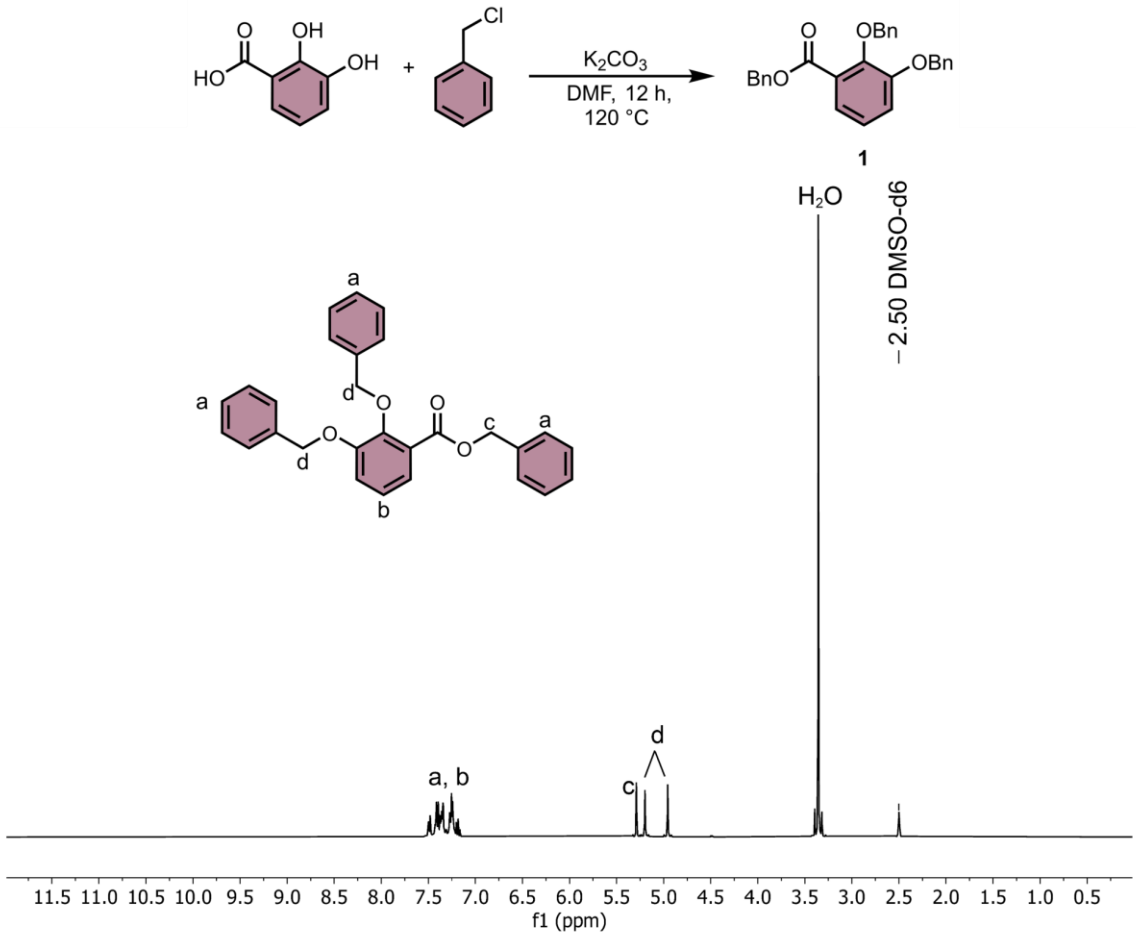

Figure S1. Synthesis and ^{1}H NMR spectra of compound 1.

^{1}H NMR (400 MHz, DMSO-D_6) δ 7.51 – 7.47 (m, 2H), 7.44 – 7.31 (m, 9H), 7.29 – 7.16 (m, 7H), 5.29 (s, 2H), 5.20 (s, 2H), 4.96 (s, 2H)

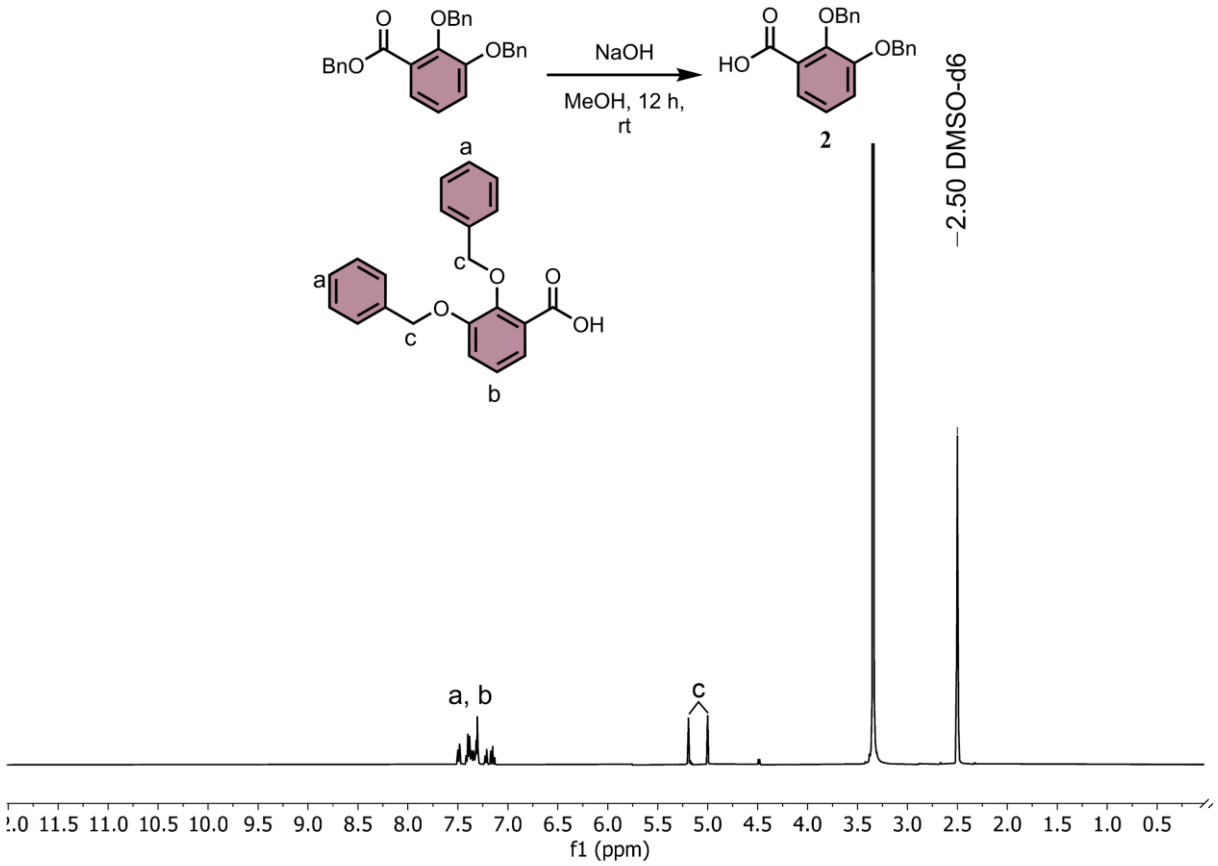

Figure S2. Synthesis and ^{1}H NMR spectra of compound 2.

^{1}H NMR (400 MHz, DMSO-D_6) δ 7.53 – 7.46 (m, 2H), 7.44 – 7.27 (m, 9H), 7.25 – 7.11 (m, 2H), 5.19 (s, 2H), 5.00 (s, 2H).

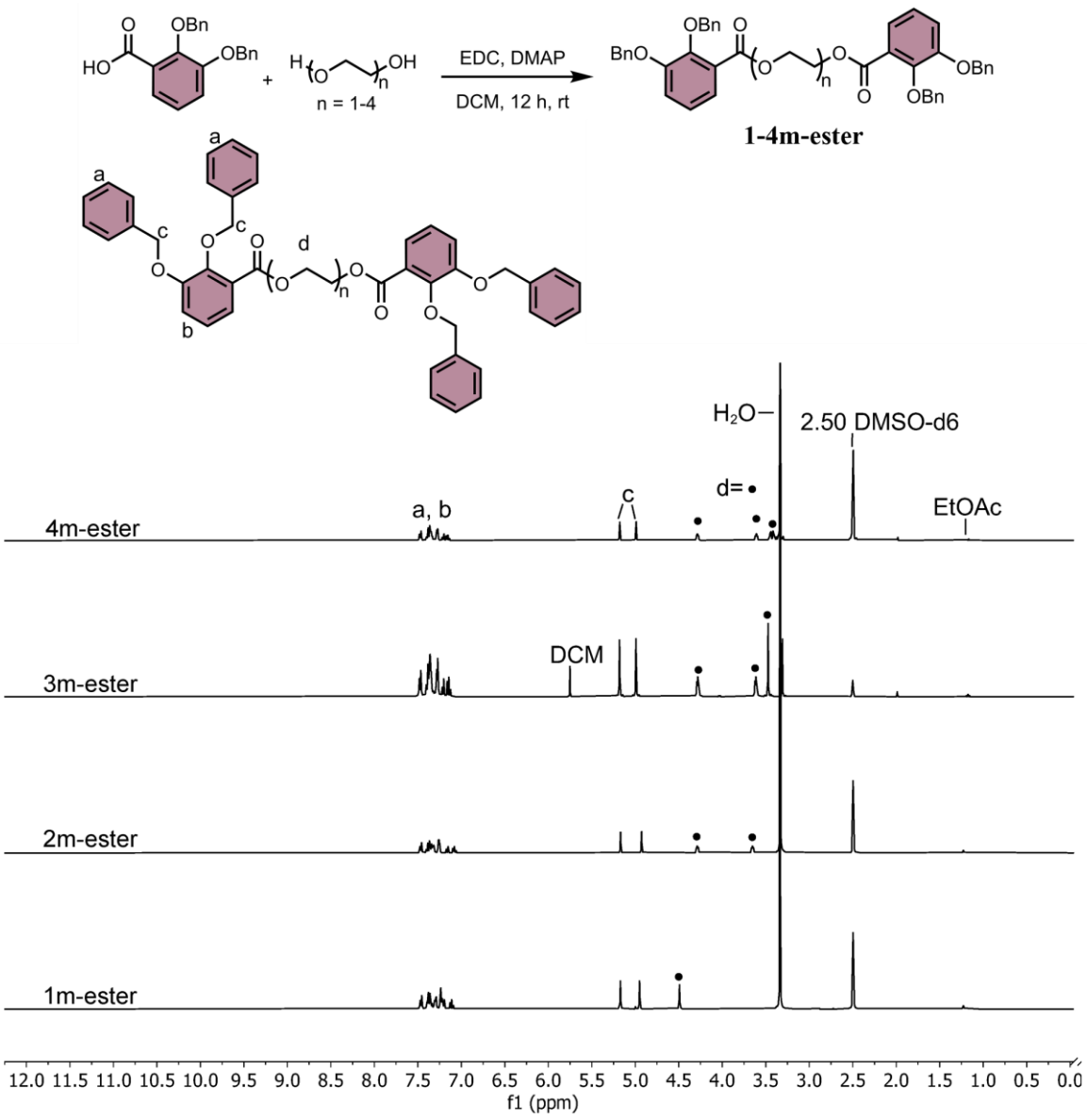

Figure S3. Synthesis and ^{1}H NMR spectra of 1-4m-ester, n-series.

1m-ester: ^{1}H NMR (400 MHz, DMSO-D_6) δ 7.45 – 7.40 (m, 4H), 7.37 – 7.23 (m, 12H), 7.23 – 7.14 (m, 8H), 7.07 (t, J = 8.0 Hz, 2H), 5.13 (s, 4H), 4.91 (s, 4H), 4.45 (s, 4H).

2m-ester: ^{1}H NMR (400 MHz, DMSO-D_6) δ 7.43 (d, J = 7.2 Hz, 4H), 7.37 – 7.27 (m, 12H), 7.24 – 7.20 (m, 6H), 7.14 – 7.11 (m, 2H), 7.04 (t, J = 8.0 Hz, 2H), 5.13 (s, 4H), 4.89 (s, 4H), 4.27 – 4.22 (m, 4H), 3.61 (t, J = 4.7 Hz, 4H).

3m-ester: ^{1}H NMR (400 MHz, DMSO-D_6) δ 7.46 – 7.41 (m, 4H), 7.37 – 7.21 (m, 18H), 7.17 (dd, J = 7.9, 1.6 Hz, 2H), 7.11 (t, J = 7.9 Hz, 2H), 5.14 (s, 4H), 4.95 (s, 4H), 4.24 (t, 4H), 3.58 (t, 4H), 3.44 (s, 4H).

4m-ester: ^{1}H NMR (400 MHz, DMSO-D_6) δ 7.46 – 7.41 (m, 4H), 7.39 – 7.20 (m, 18H), 7.17 (dt, J = 7.9, 1.5 Hz, 2H), 7.12 (td, J = 7.9, 1.2 Hz, 2H), 5.14 (s, 4H), 4.95 (s, 4H), 4.25 (dd, J = 5.6, 3.7 Hz, 4H), 3.57 (dd, J = 5.5, 3.7 Hz, 4H), 3.41 (dd, J = 6.3, 3.2 Hz, 4H), 3.39 – 3.35 (m, 4H).

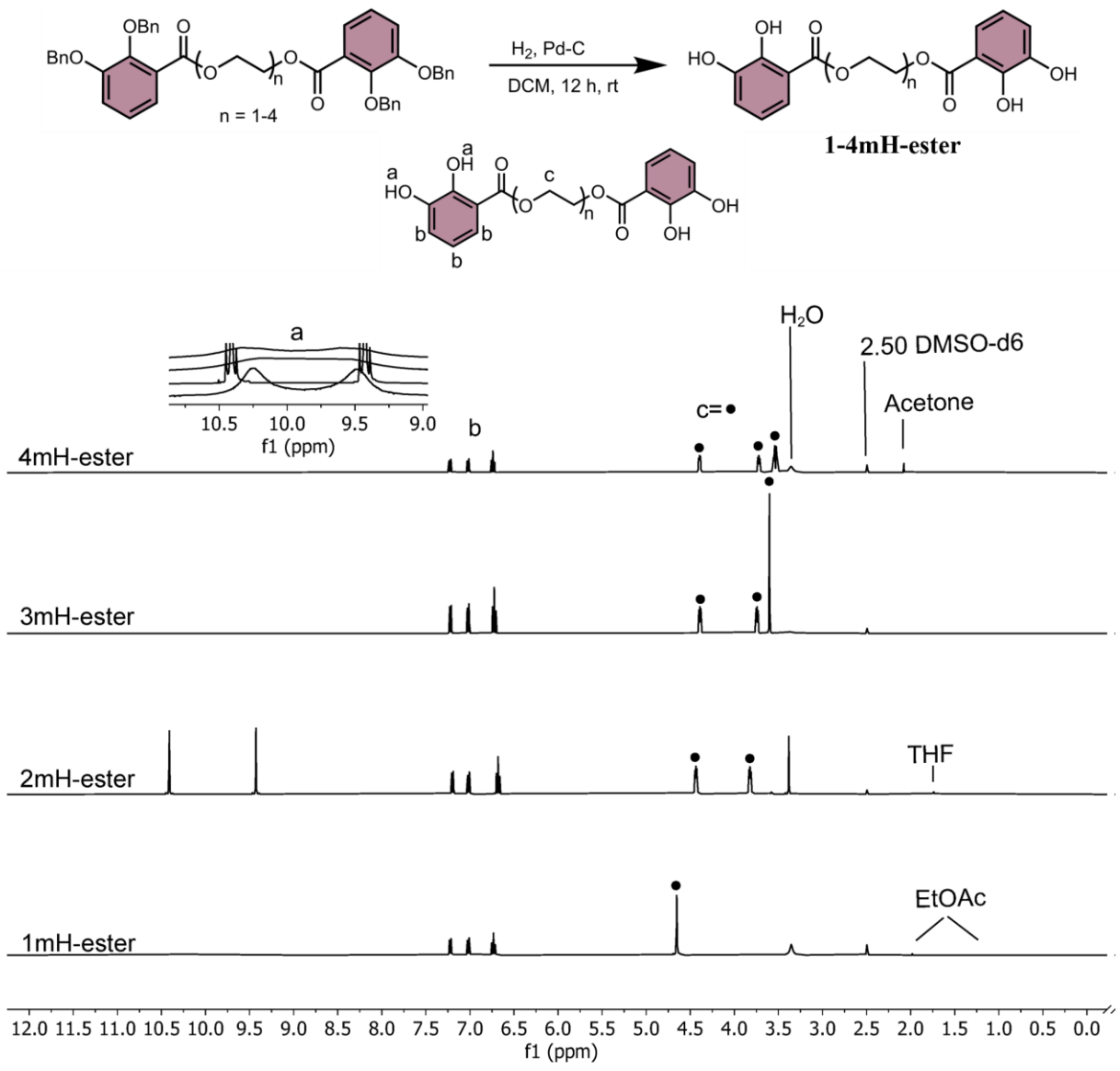

Figure S4. Synthesis and ^{1}H NMR spectra of 1-4mH-ester, n-series.

1mH-ester: ^{1}H NMR (400 MHz, DMSO-D_6) δ 10.25 (s, 2H), 9.49 (s, 2H), 7.23 (dt, J = 8.1, 1.3 Hz, 2H), 7.02 (dt, J = 7.8, 1.3 Hz, 2H), 6.74 (td, J = 7.9, 0.9 Hz, 2H), 4.66 (s, 4H).

2mH-ester: ^{1}H NMR (400 MHz, DMSO-D_6) δ 10.42 (s, 2H), 9.43 (s, 2H), 7.20 (dd, J = 8.1, 1.6 Hz, 2H), 7.02 (dd, J = 7.9, 1.6 Hz, 2H), 6.69 (t, J = 7.9 Hz, 2H), 4.44 (t, 4H), 3.83 (t, 4H).

3mH-ester: ^{1}H NMR (400 MHz, DMSO-D_6) δ 10.15 (s, 2H), 9.66 (s, 2H), 7.22 (dd, J = 8.0, 1.6 Hz, 2H), 7.02 (dd, J = 7.9, 1.6 Hz, 2H), 6.73 (t, J = 7.9 Hz, 2H), 4.43 – 4.36 (m, 4H), 3.78 – 3.71 (m, 4H), 3.60 (s, 4H).

4mH-ester: ^{1}H NMR (400 MHz, DMSO-D_6) δ 10.28 (s, 2H), 9.54 (s, 2H), 7.23 (dd, J = 8.0, 1.5 Hz, 2H), 7.02 (dd, J = 7.8, 1.5 Hz, 2H), 6.74 (t, J = 7.9 Hz, 2H), 4.40 (t, 4H), 3.73 (t, 4H), 3.62 – 3.47 (m, 8H).

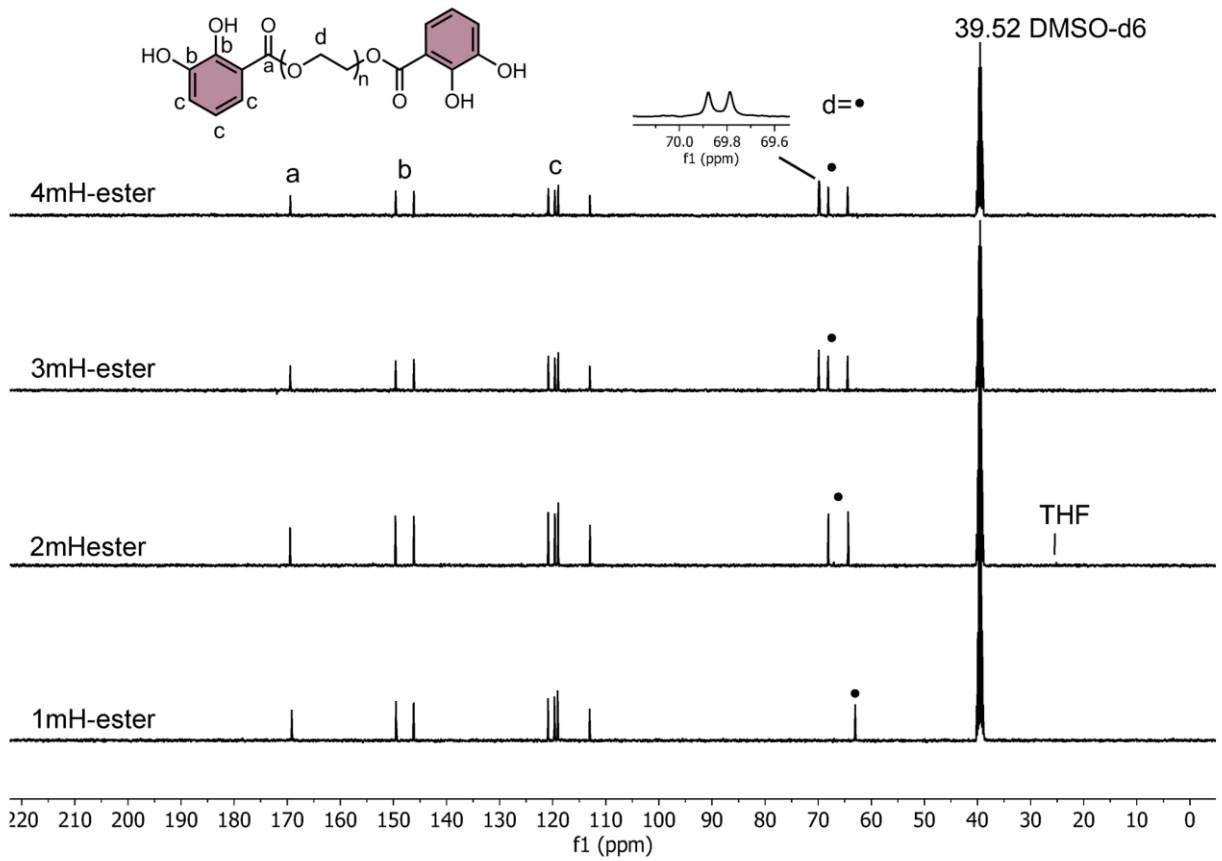

Figure S5. ^{13}C NMR spectra of 1-4mH-ester, n-series.

1mH-ester:^{13}C NMR (101 MHz, DMSO-D_6) δ 169.15, 149.49, 146.19, 120.88, 119.68, 119.07, 113.07, 63.01.

2mH-ester:^{13}C NMR (101 MHz, DMSO-D_6) δ 169.45, 149.63, 146.14, 120.85, 119.58, 118.95, 112.97, 68.08, 64.38.

3mH-ester: ^{13}C NMR (101 MHz, DMSO-D_6) δ 169.40, 149.58, 146.14, 120.83, 119.60, 118.96, 113.01, 69.88, 68.14, 64.45.

4mH-ester: ^{13}C NMR (101 MHz, DMSO-D_6) δ 169.39, 149.57, 146.14, 120.82, 119.61, 118.95, 113.01, 69.88, 69.79, 68.10, 64.45.

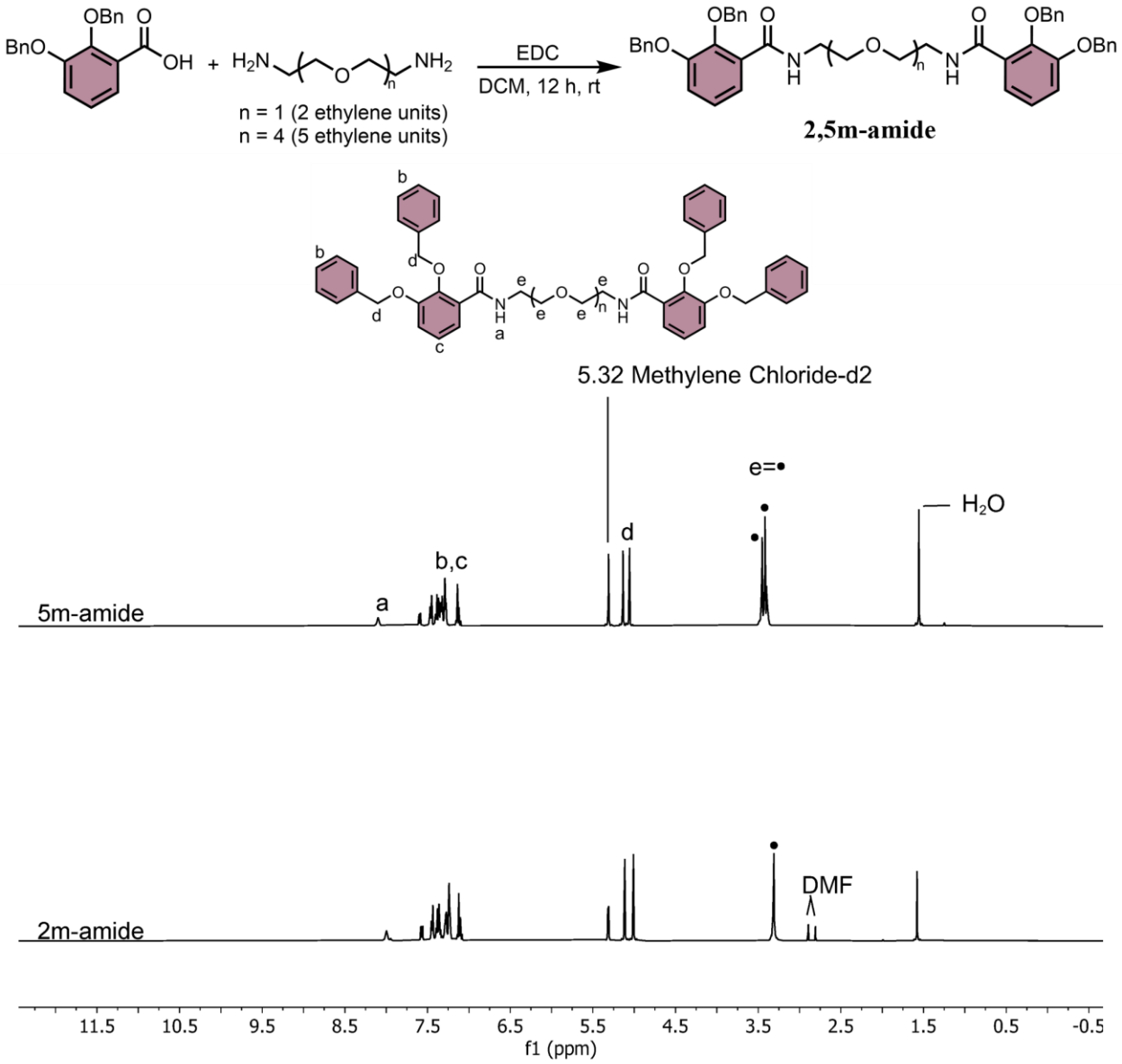

Figure S6. Synthesis and ^{1}H NMR spectra of 2,5m-amide, n-series.

2m-amide: ^{1}H NMR (400 MHz, METHYLENE-CHLORI) δ 8.01 (s, 2H), 7.58 (ddd, J = 6.9, 2.6, 1.3 Hz, 2H), 7.49 – 7.18 (m, 20H), 7.17 – 7.07 (m, 4H), 5.12 (s, 4H), 5.02 (s, 4H), 3.32 (q, J = 1.7 Hz, 8H).

5m-amide: ^{1}H NMR (400 MHz, METHYLENE-CHLORI) δ 8.11 (s, 2H), 7.61 (ddd, *J* = 6.9, 2.6, 1.1 Hz, 2H), 7.47 (dt, *J* = 7.7, 1.4 Hz, 4H), 7.43 – 7.24 (m, 15H), 7.21 – 7.08 (m, 5H), 5.15 (s, 4H), 5.07 (s, 4H), 3.49 – 3.39 (m, 20H).

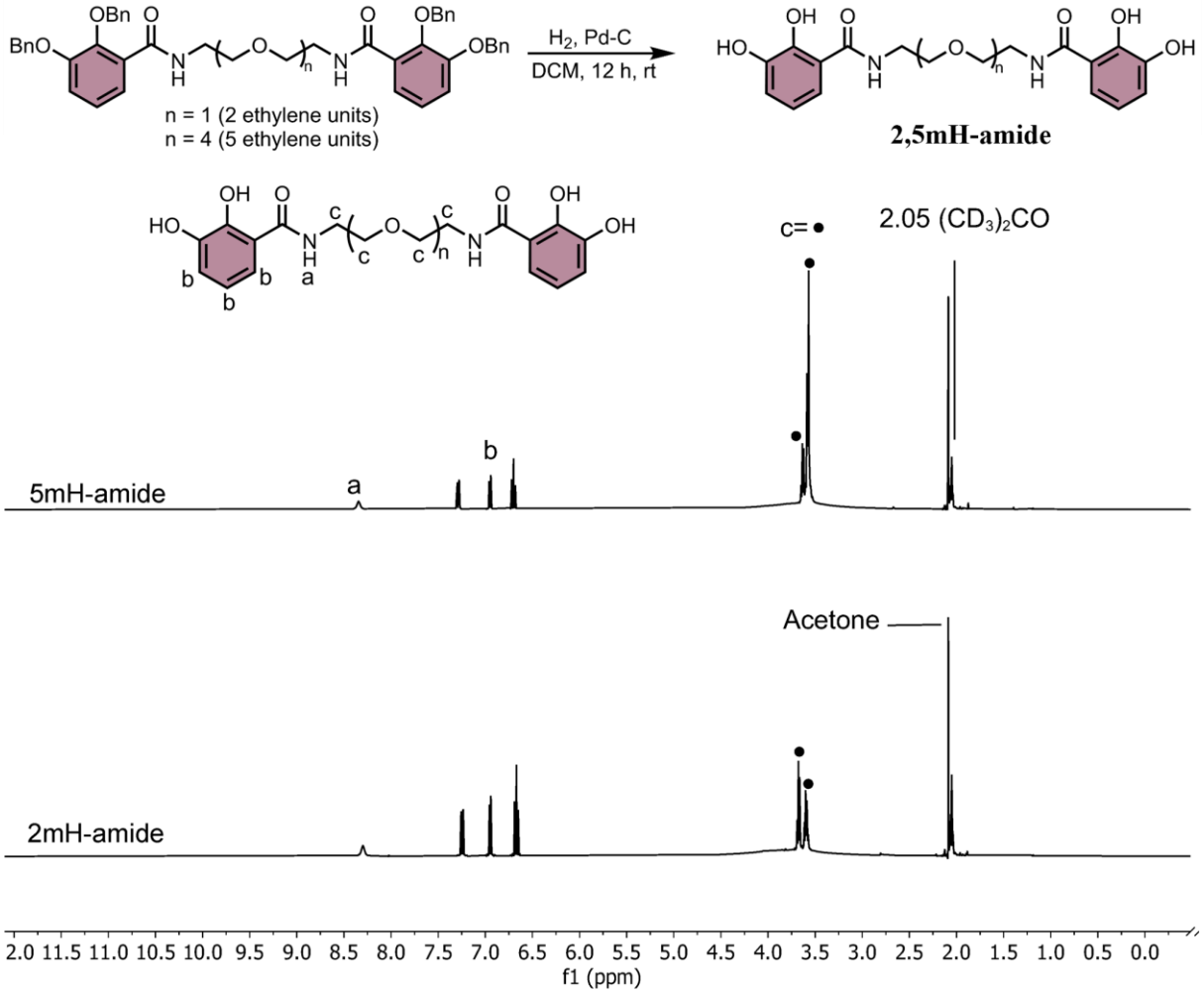

Figure S7. Synthesis and ^{1}H NMR spectra of 2,5mH-amide, n-series.

2mH-amide: ^{1}H NMR (400 MHz, ACETONE-D_6) δ 8.30 (s, 2H), 7.25 (dd, *J* = 8.1, 1.5 Hz, 2H), 6.97 – 6.93 (m, 2H), 6.67 (t, *J* = 8.0 Hz, 2H), 3.68 (dd, *J* = 5.8, 4.8 Hz, 4H), 3.62 – 3.57 (m, 4H).

5mH-amide: ^{1}H NMR (400 MHz, ACETONE-D_6) δ 8.34 (s, 2H), 7.29 (dd, *J* = 8.2, 1.4 Hz, 2H), 6.95 (dt, *J* = 7.9, 1.0 Hz, 2H), 6.73 – 6.67 (m, 2H), 3.64 (dd, *J* = 6.3, 5.0 Hz, 5H), 3.59 – 3.56 (m, 15H).

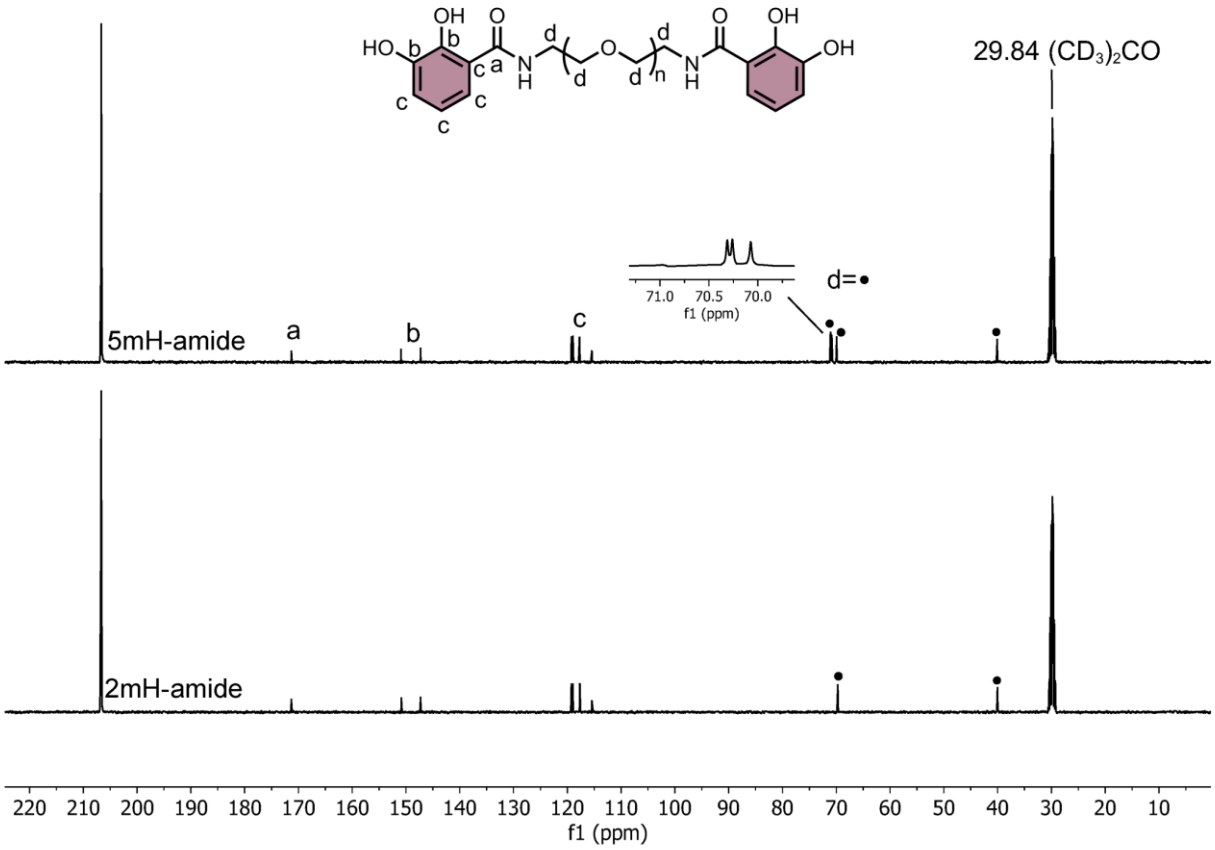

Figure S8. ^{13}C NMR spectra of 2,5mH-amide, n-series.

2mH-amide: ^{13}C NMR (101 MHz, ACETONE-D_6) δ 206.68, 119.25, 118.97, 117.68, 69.70, 40.02.

5mH-amide: ^{13}C NMR (101 MHz, ACETONE-D_6) δ 206.66, 119.24, 118.94, 117.74, 71.08, 71.02, 70.84, 69.92, 40.09.

High-Resolution Mass Spectrometry (HRMS) Data

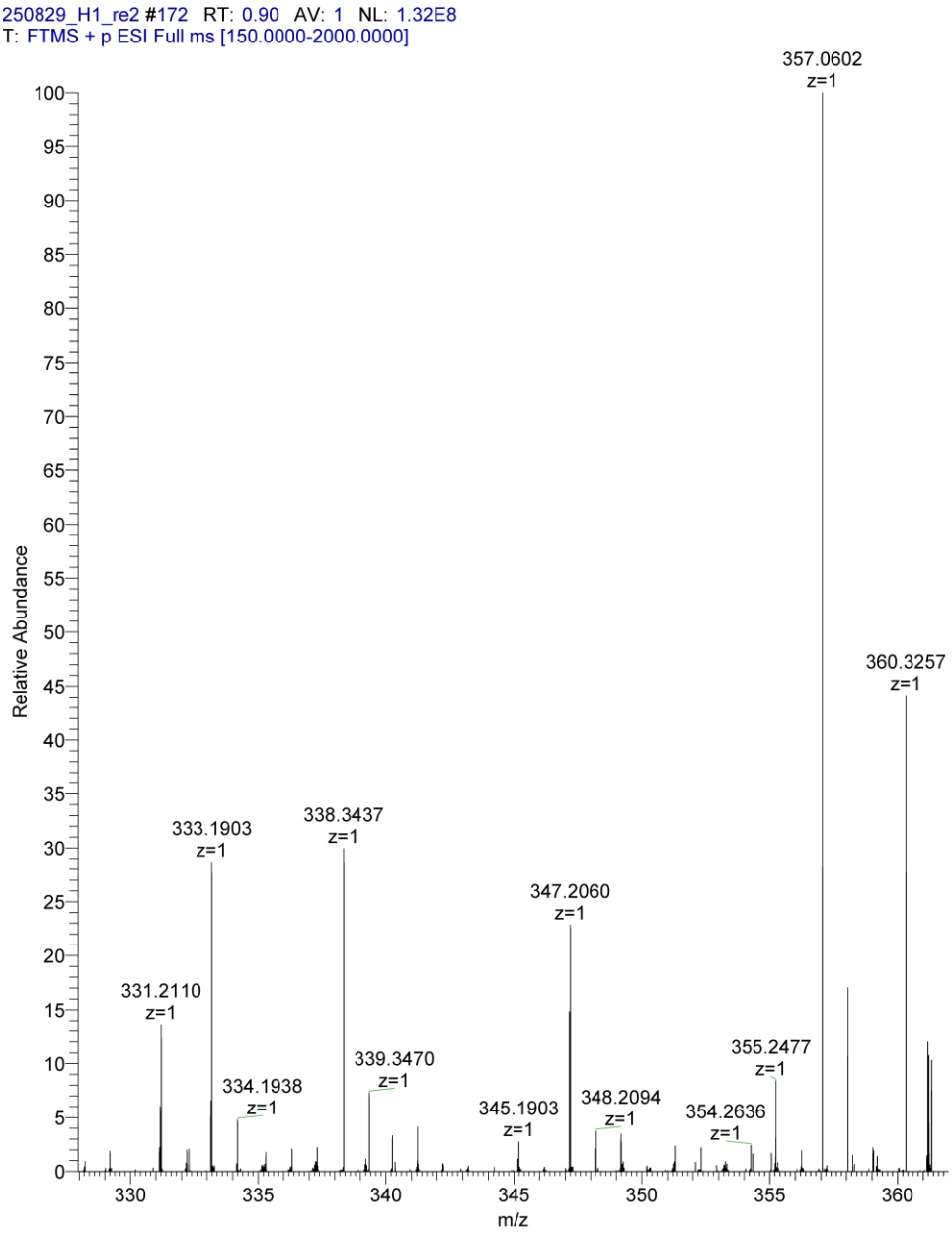

Figure S9. HRMS (ESI) spectrum of 1mH-ester. $[M+Na]^+$ calcd for $C_{16}H_{14}O_8Na$, 357.0582; found, 357.0602 (Δ = 5.5 ppm).

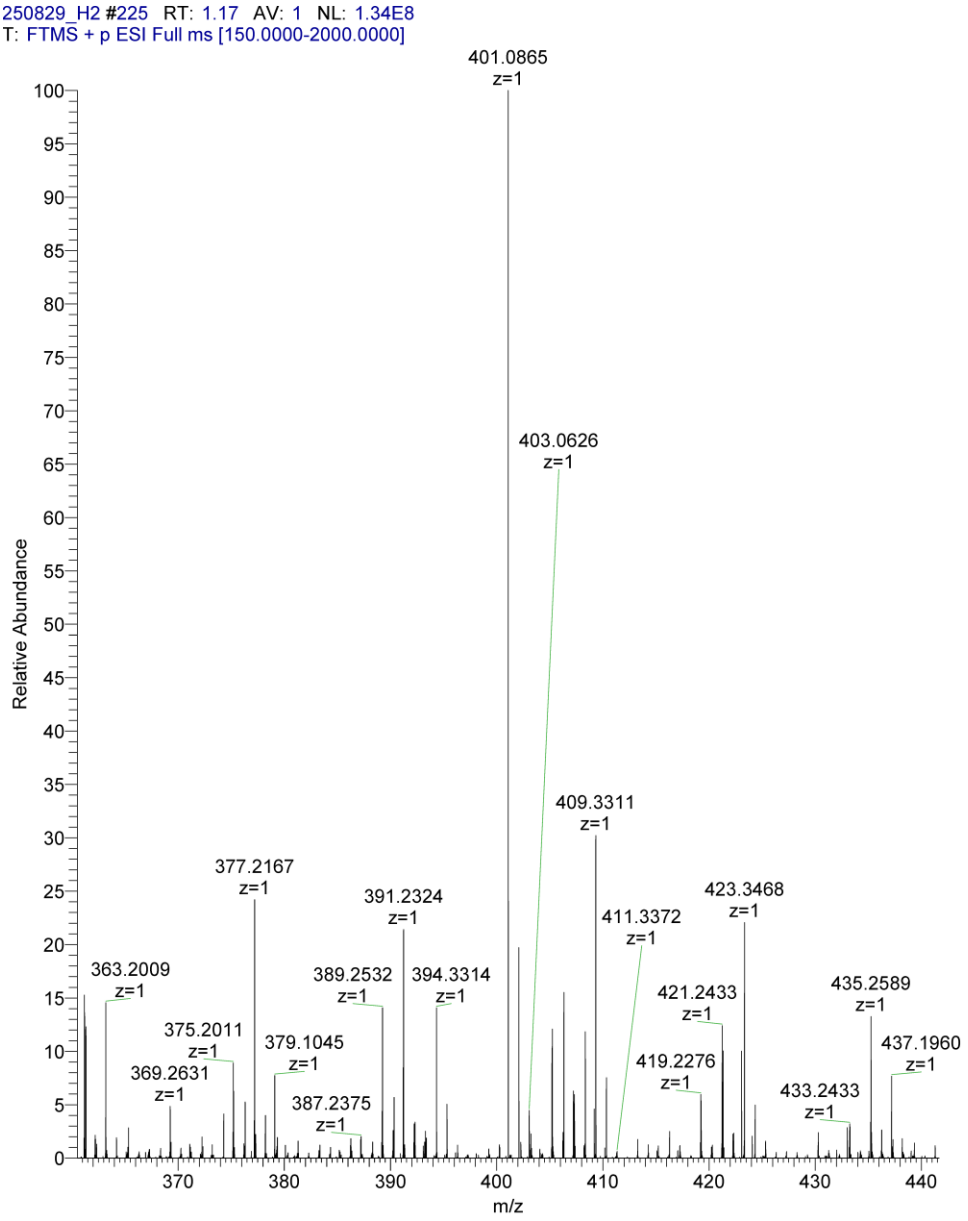

Figure S10. HRMS (ESI) spectrum of 2mH-ester. $[M+Na]^+$ calcd for $C_{18}H_{18}O_9Na$, 401.0849; found, 401.0865 (Δ = 4.1 ppm).

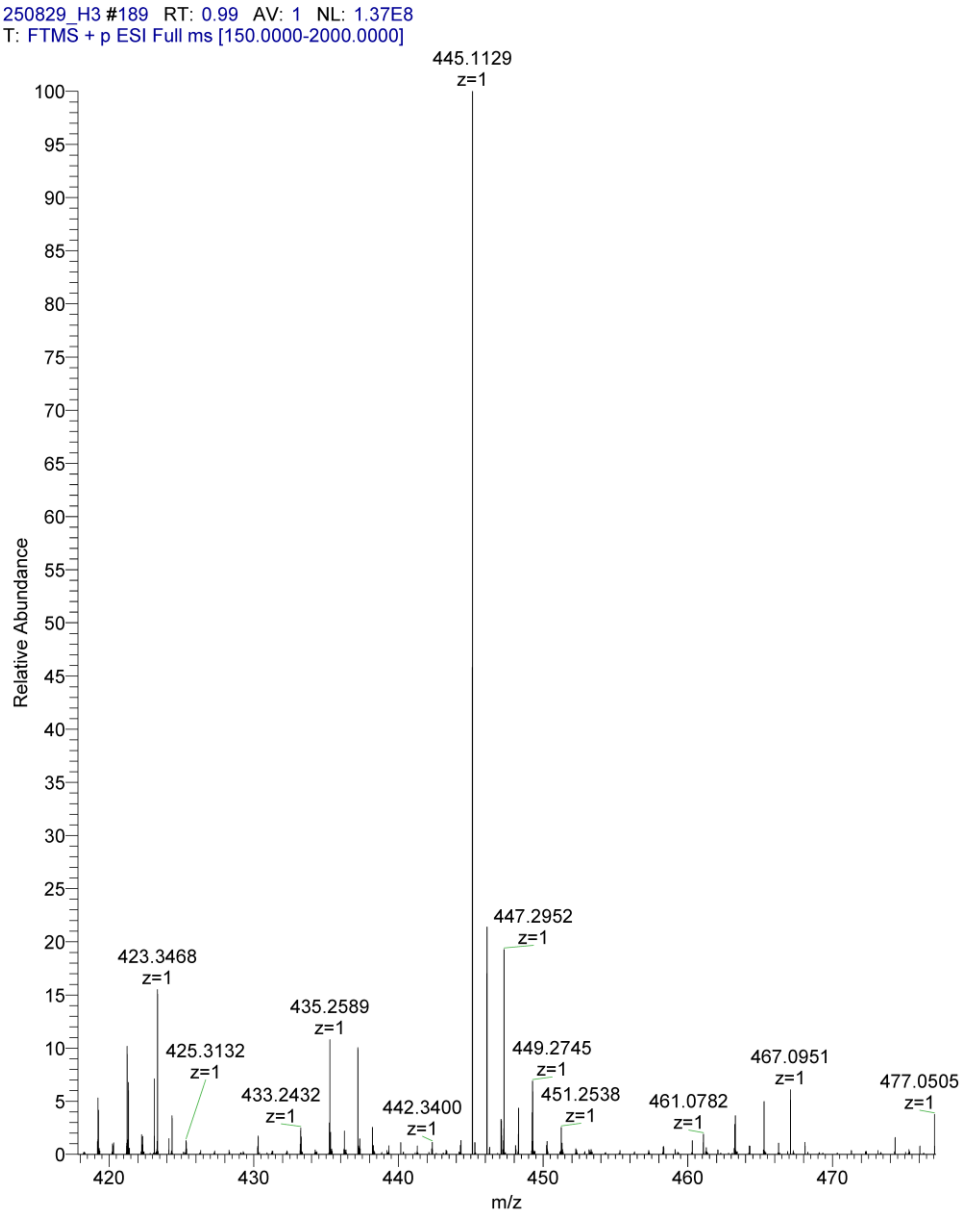

Figure S11. HRMS (ESI) spectrum of 3mH-ester. $[M+Na]^+$ calcd for $C_{20}H_{22}O_{10}Na$, 445.1101; found, 445.1129 (Δ = 6.4 ppm).

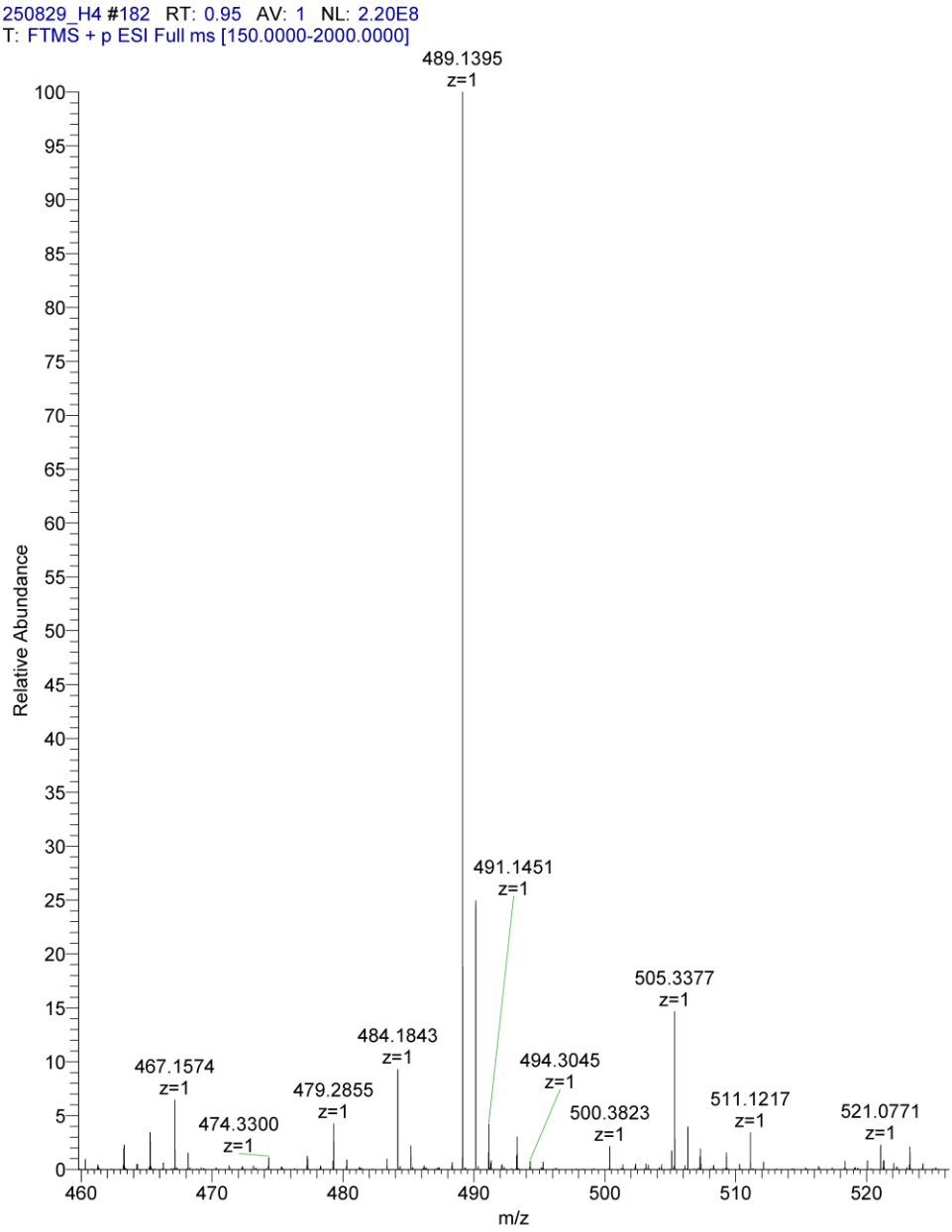

Figure S12. HRMS (ESI) spectrum of 4mH-ester. $[M+Na]^+$ calcd for $C_{22}H_{26}O_{11}Na$, 489.1373; found, 489.1395 (Δ = 4.5 ppm).

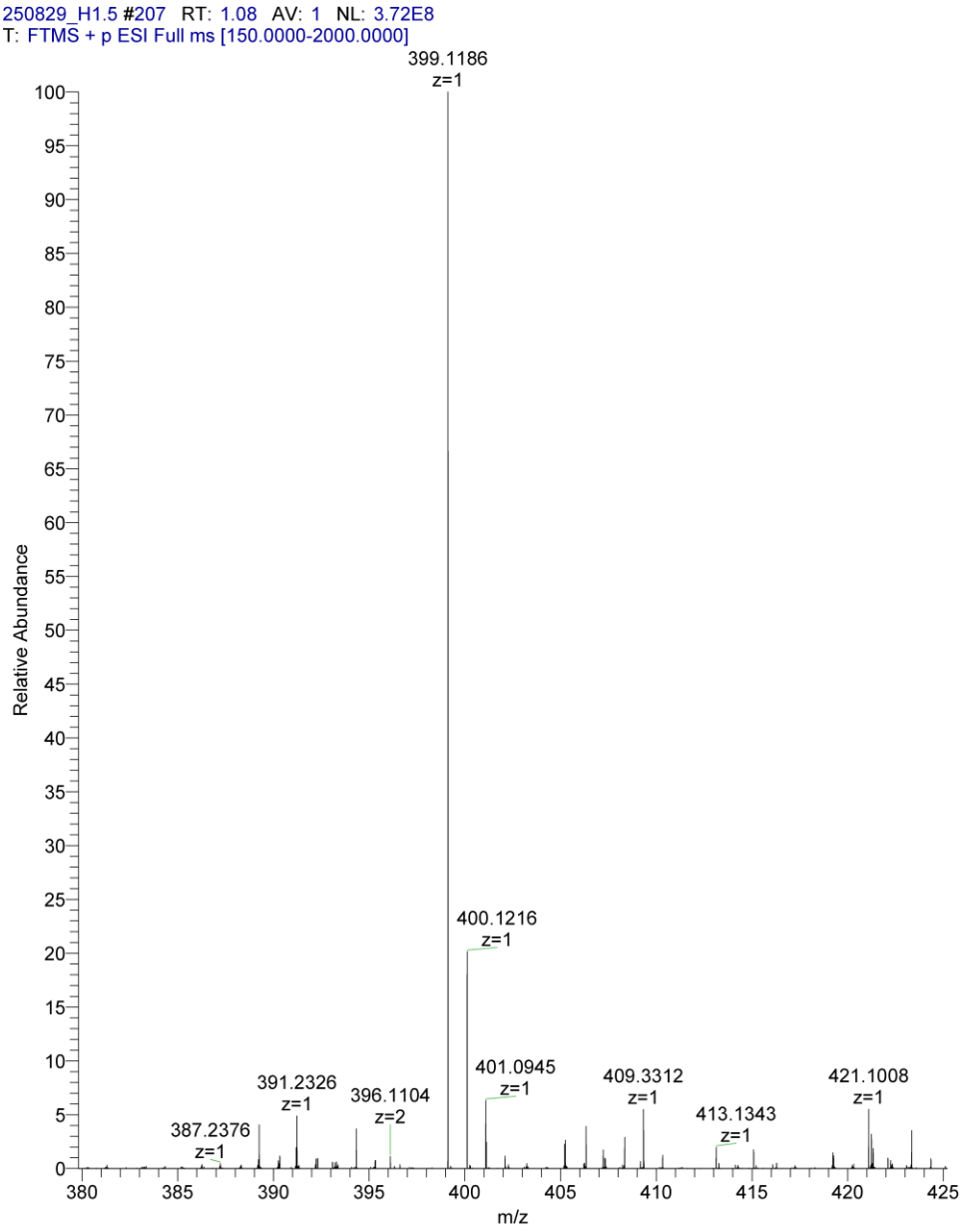

Figure S13. HRMS (ESI) spectrum of 2mH-amide. $[M+Na]^+$ calcd for $C_{18}H_{20}N_2O_7Na$, 399.1167; found, 399.1186 (Δ = 4.7 ppm).

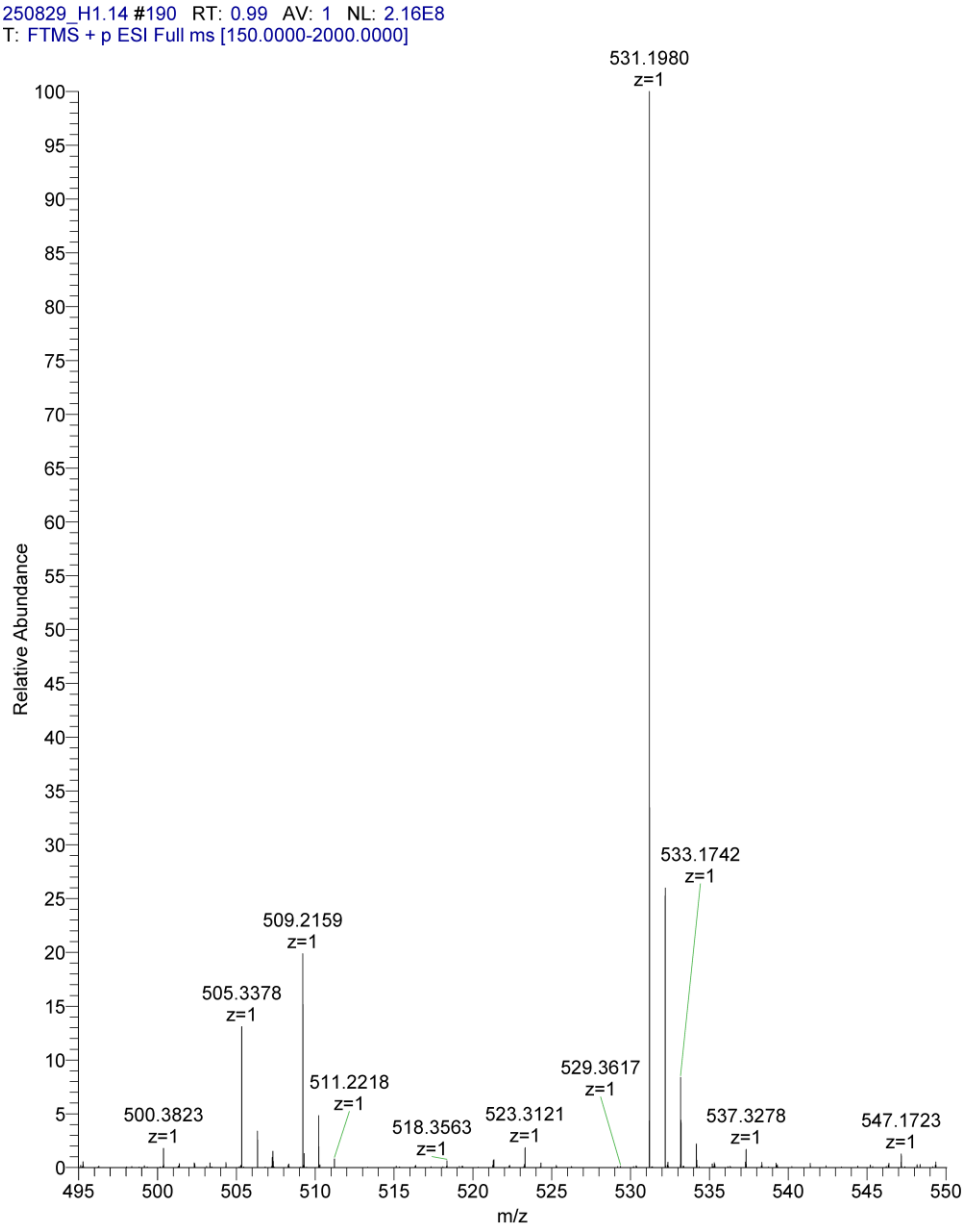

Figure S14. HRMS (ESI) spectrum of 5mH-amide. $[M+Na]^+$ calcd for $C_{24}H_{32}N_2O_{10}Na$, 531.1955; found, 531.1980 (Δ = 4.8 ppm).

Synthesis of gels

Scheme S1. Synthesis of 2,5p-amide-M^{3+} n-series.

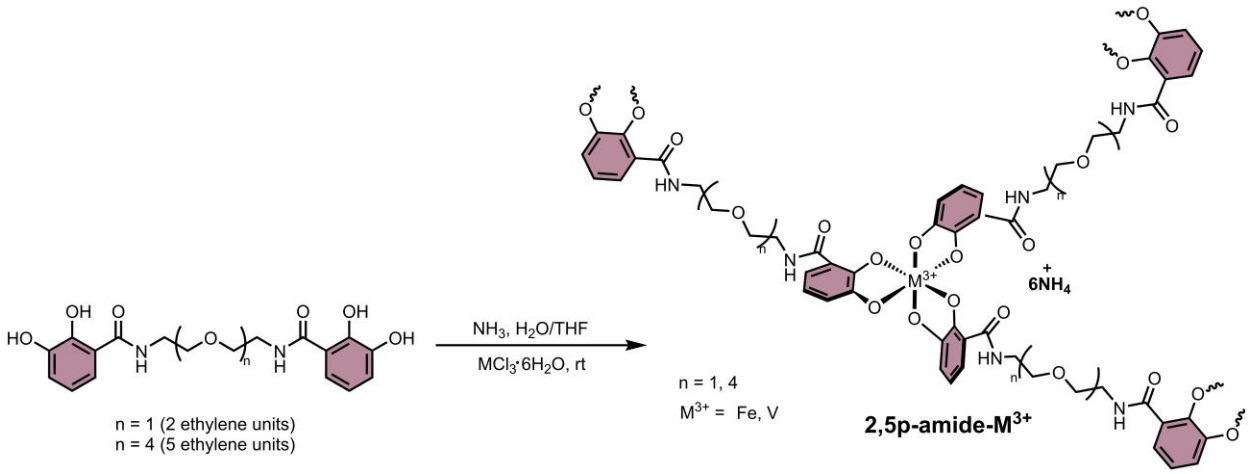

Electron Paramagnetic Resonance Spectroscopy.

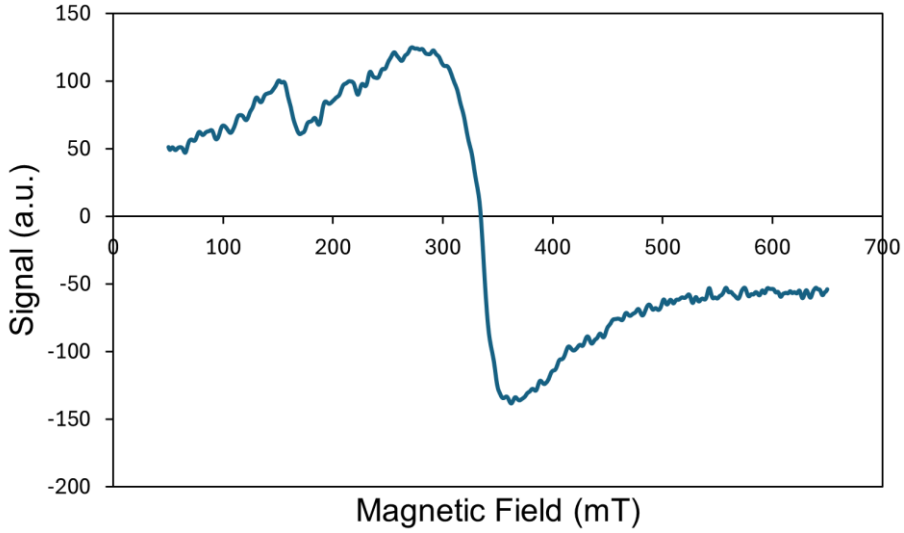

Figure S15. Room-temperature Electron Paramagnetic Resonance of 1p-ester-Fe.

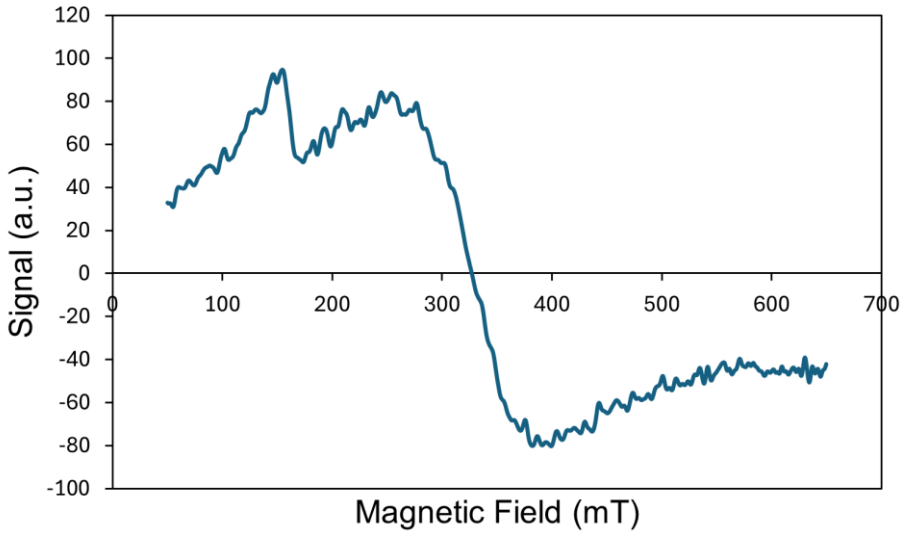

Figure S16. Room-temperature Electron Paramagnetic Resonance of 2p-ester-Fe.

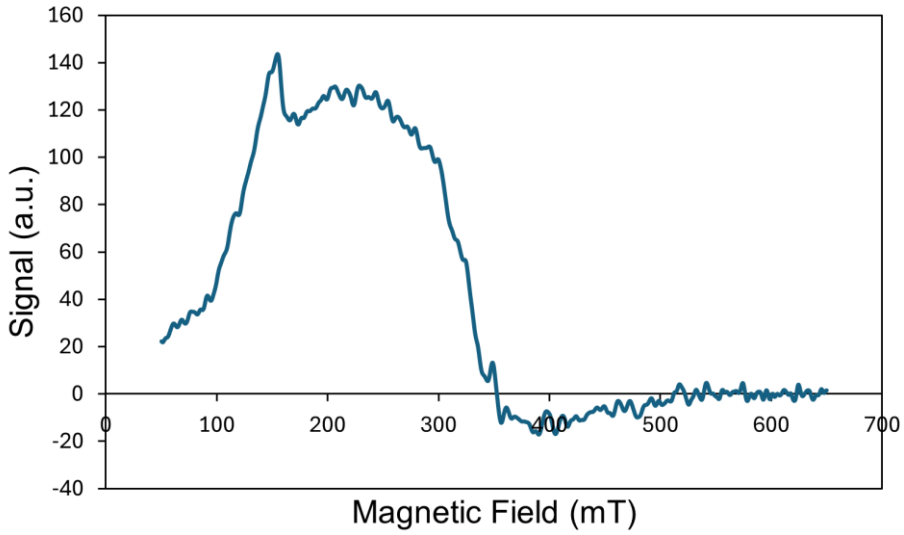

Figure S17. Room-temperature Electron Paramagnetic Resonance of 3p-ester-Fe.

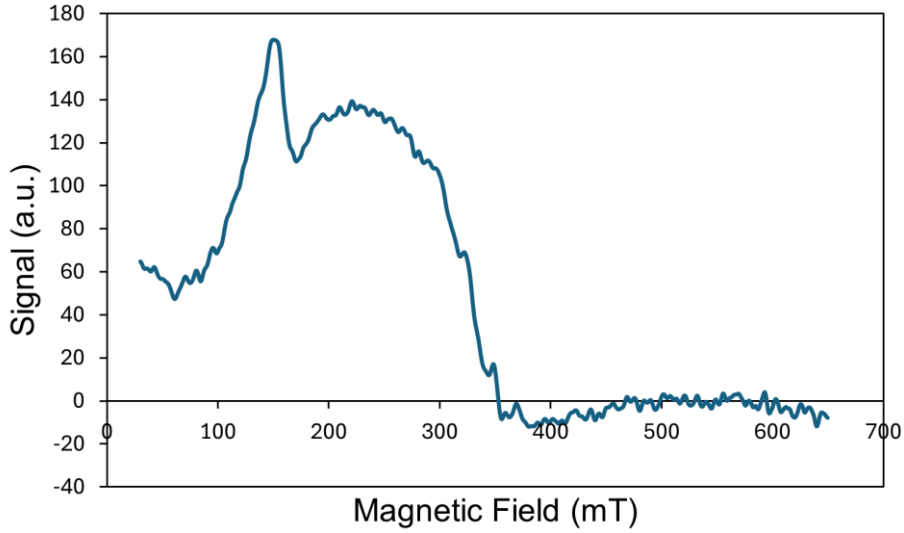

Figure S18. Room-temperature Electron Paramagnetic Resonance of 4p-ester-Fe.

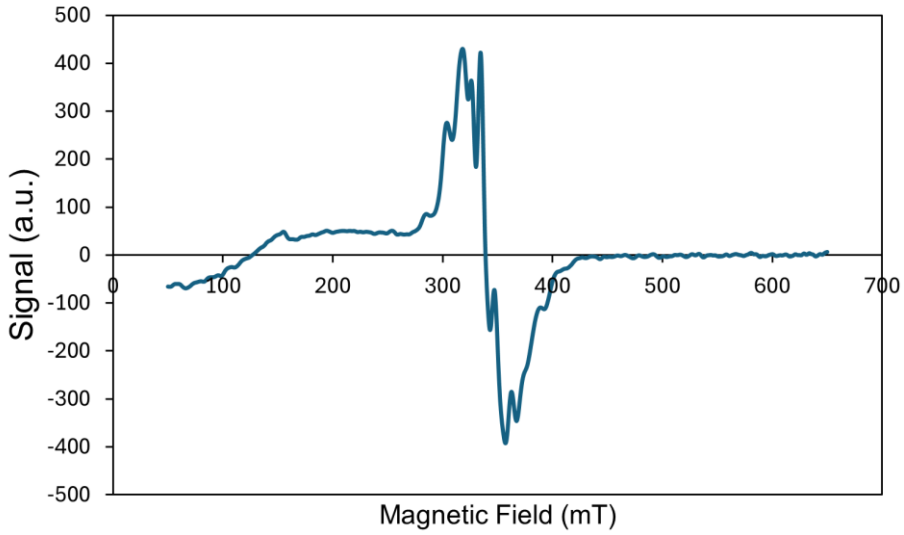

Figure S19. Room-temperature Electron Paramagnetic Resonance of 1p-ester-V.

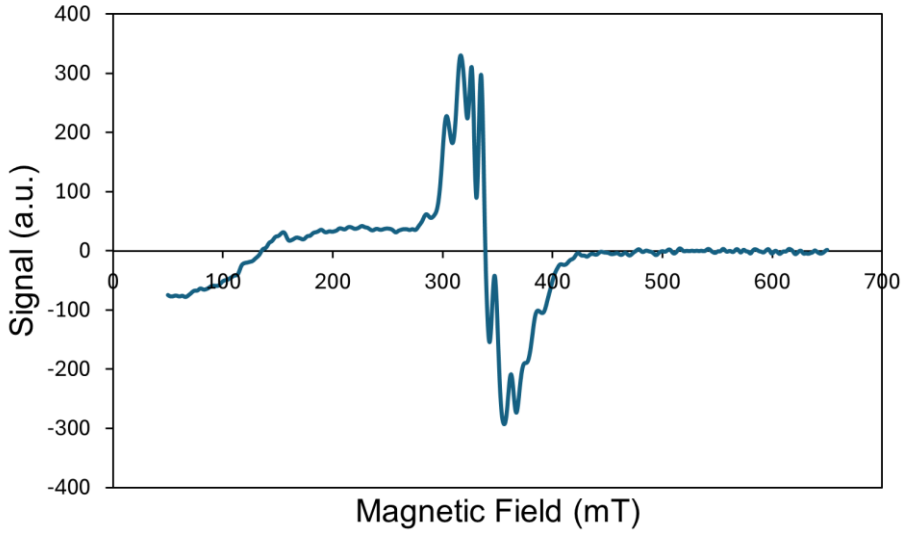

Figure S20. Room-temperature Electron Paramagnetic Resonance of 2p-ester-V.

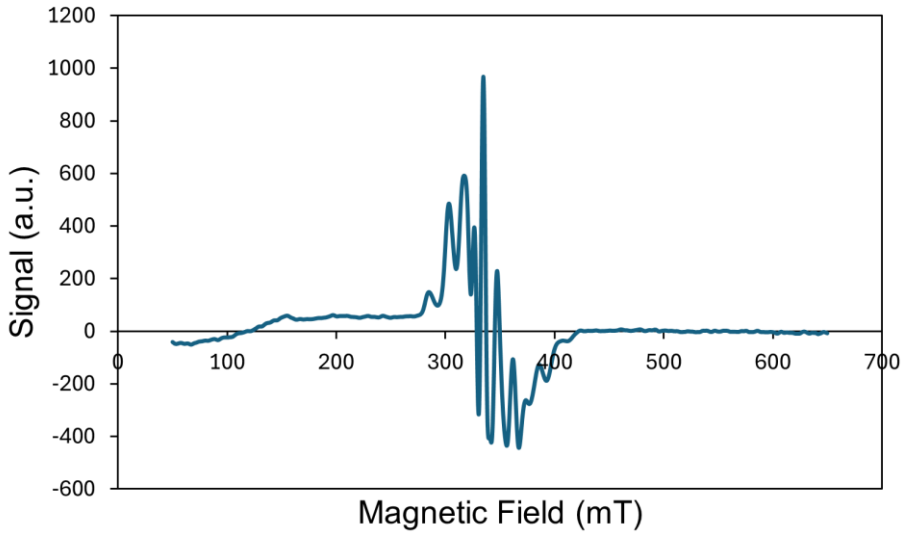

Figure S21. Room-temperature Electron Paramagnetic Resonance of 3p-ester-V.

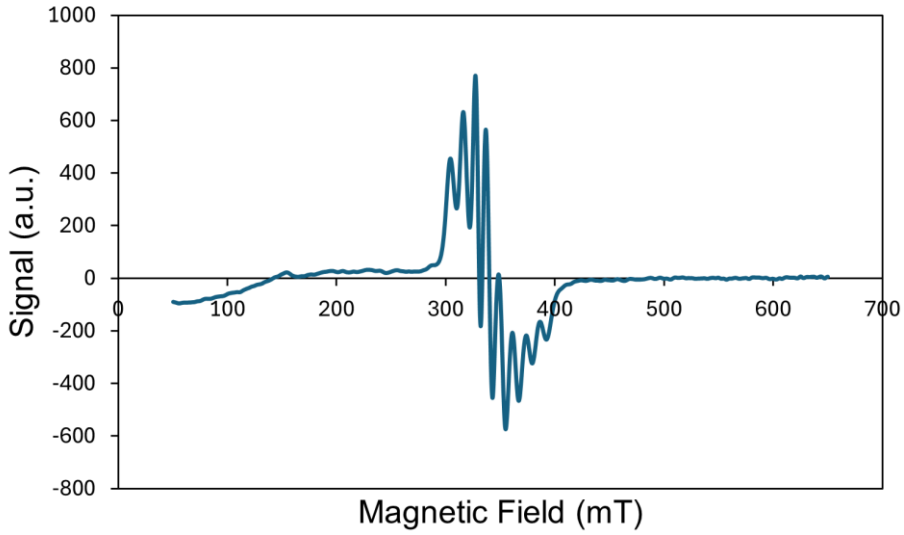

Figure S22. Room-temperature Electron Paramagnetic Resonance of 4p-ester-V.

^{57}Fe Mössbauer Spectrum.

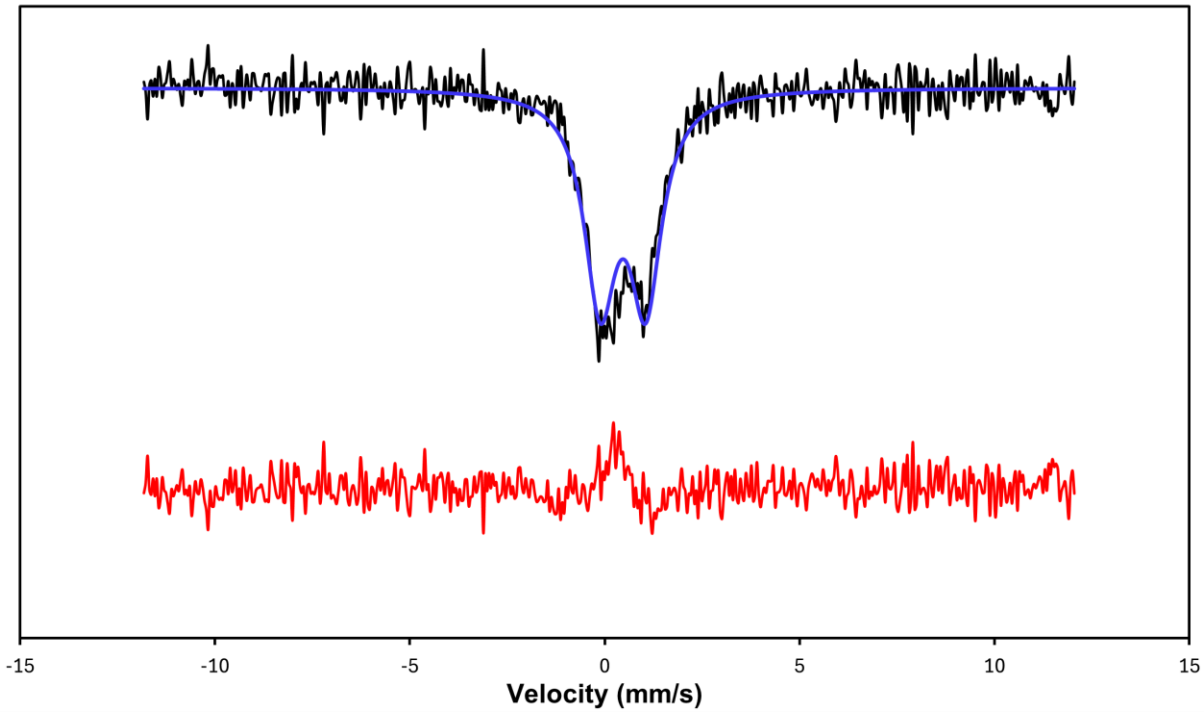

Figure S23. Room-temperature Mössbauer spectrum of 1p-ester-Fe. Experimental data in black, fit in blue, residuals in red.

Thermogravimetric Analysis (TGA) and Differential Scanning Calorimetry (DSC).

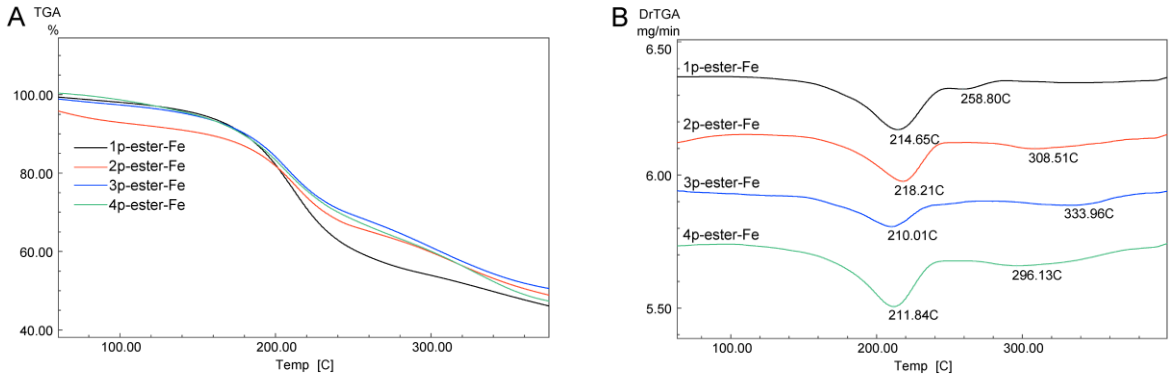

Figure S24. TGA and 1st derivative of polymers from esters Fe, A, and B, respectively.

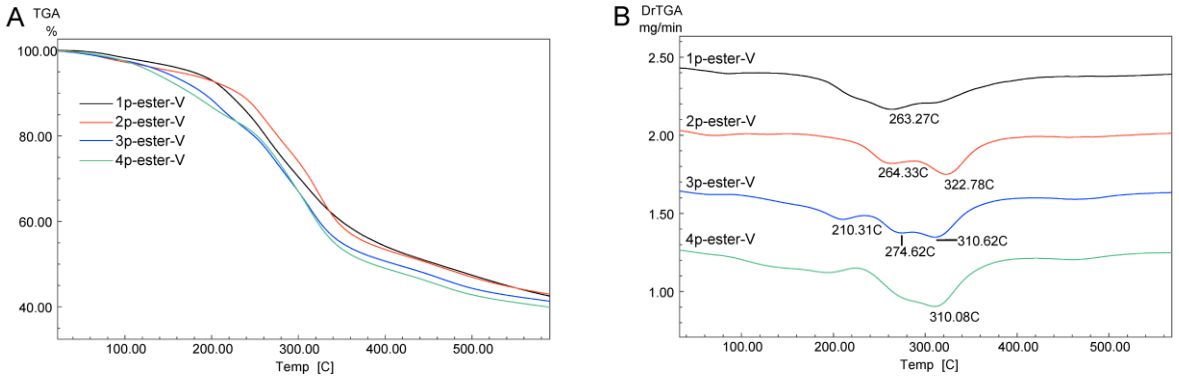

Figure S25. TGA and 1st derivative of polymers from esters using V, A, and B respectively.

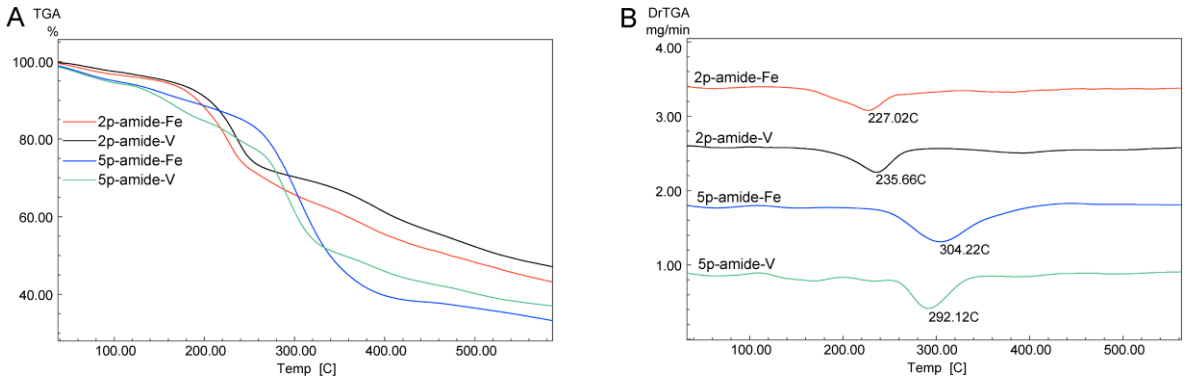

Figure S26. TGA and 1st derivative of amides using Fe and V, (A) and (B) respectively.

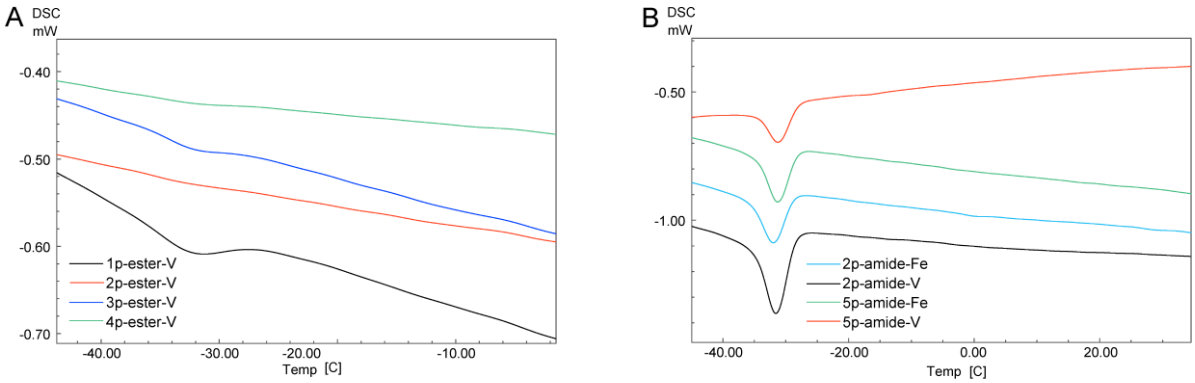

Figure S27. DSC comparison of polymers from esters using V (A) and materials from amides using Fe and V (B).

Rheology

Strain sweep

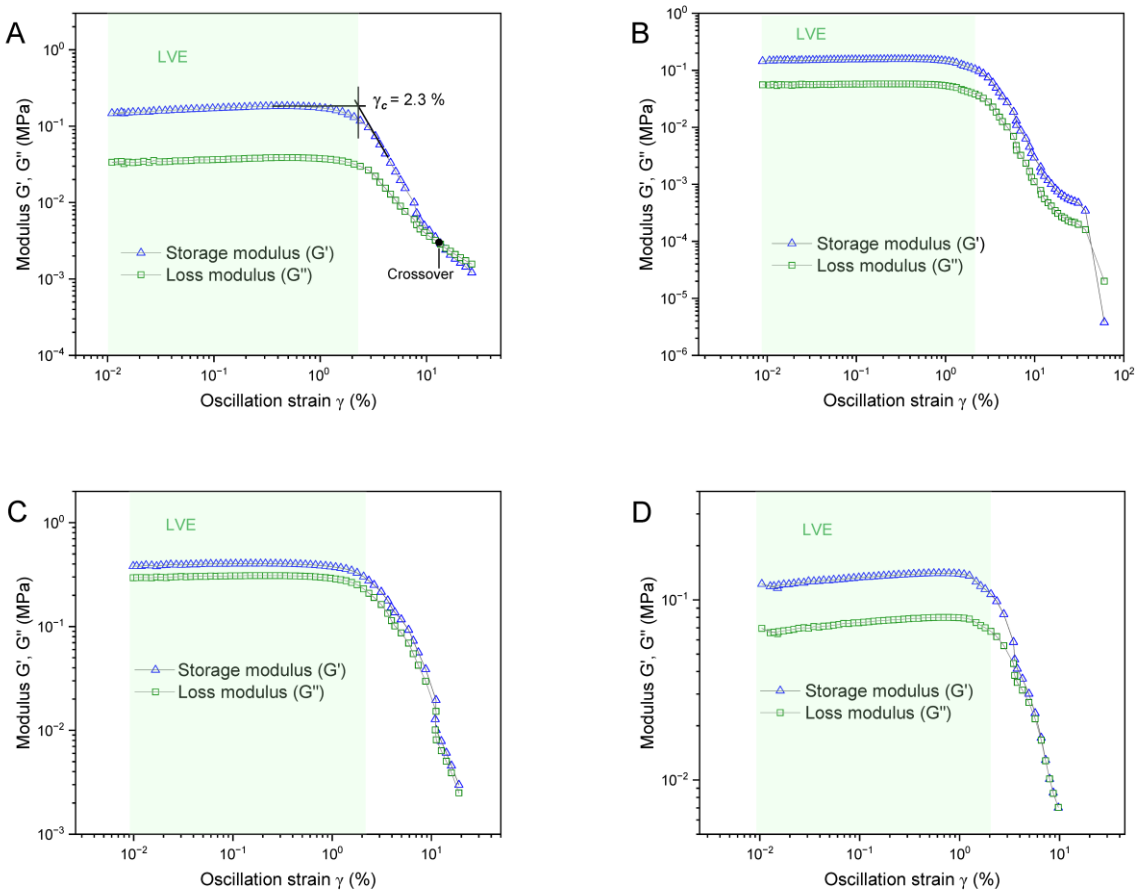

Figure S28. Strain dependence of storage modulus (G') and loss modulus (G") for Fe-catechol gels at 25 °C: A-D/1-4p-ester-Fe. (ω = 6.28 rad/s). The LVE is maintained up to ~2 % strain, after which G′ decreases, and a crossover with G″ is observed at ~14, 43, 11, and 4 % strain respectively.

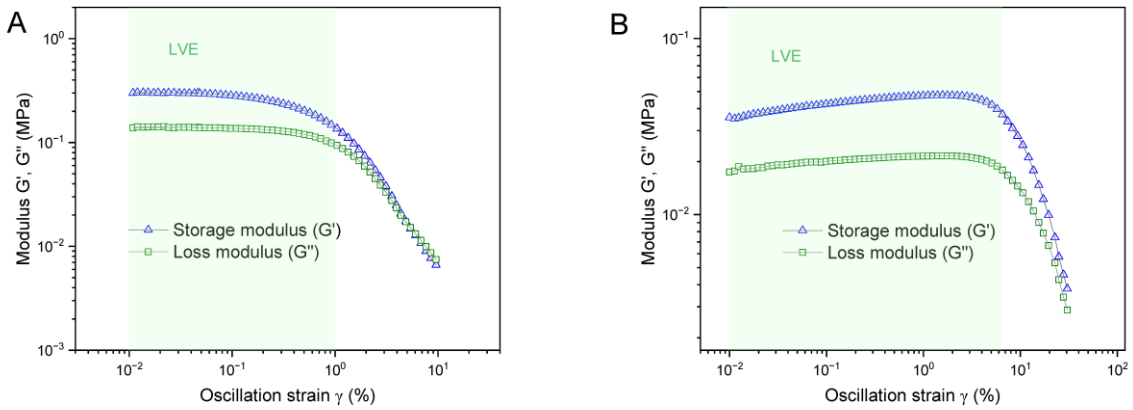

Figure S29. Strain dependence of storage modulus (G') and loss modulus (G") for Fe-catechol gels at 25 °C: A-B/2,5p-amide-Fe. (ω = 6.28 rad/s). The LVE is maintained up to

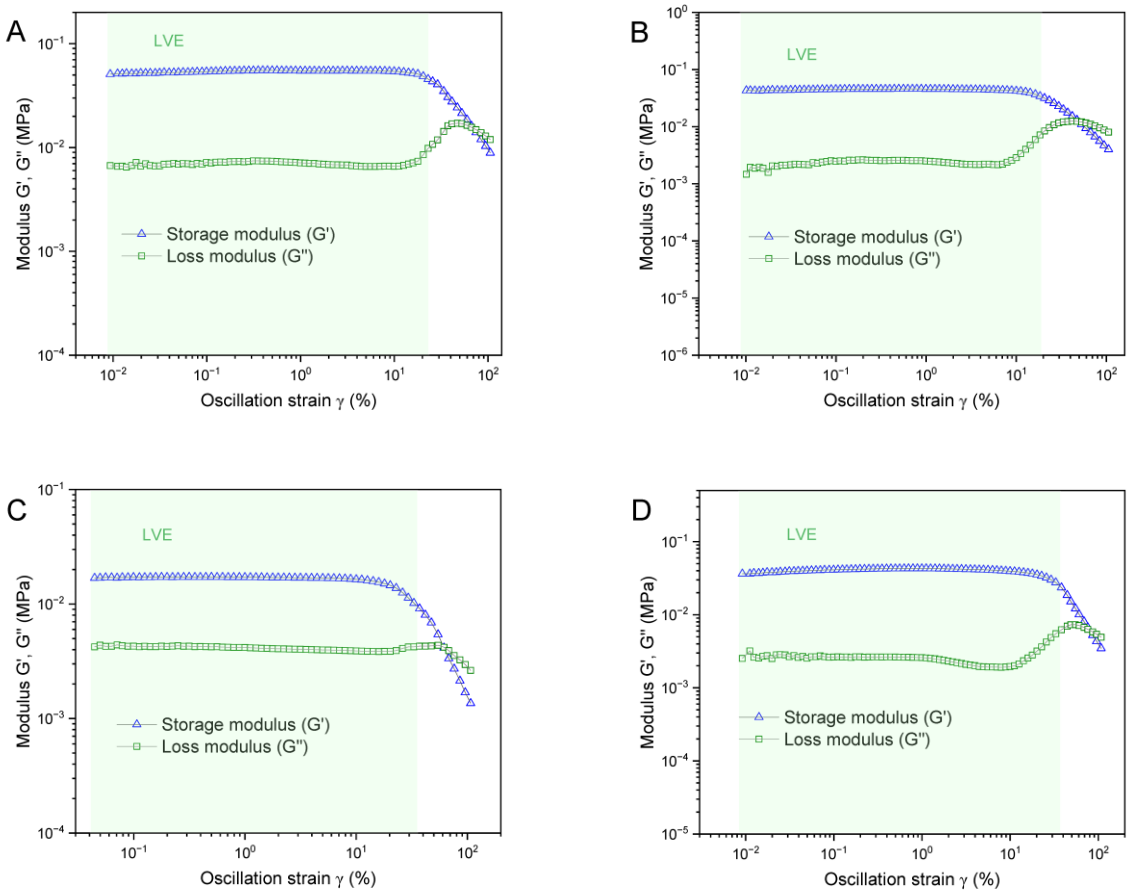

Figure S30. Strain dependence of storage modulus (G') and loss modulus (G") for V-catechol gels at 25 °C: A-D/1-4p-ester-V. (ω = 6.28 rad/s). The LVE is maintained up to ~22, 19, 33, and 31 % strain respectively, after which G′ decreases, and a crossover with G″ is observed at 67, 53, 62, and 76 % respectively.

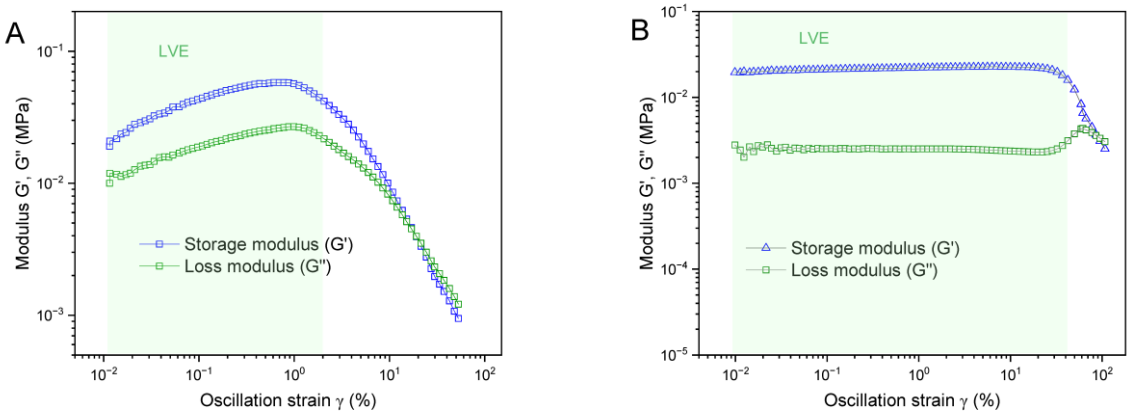

Figure S31. Strain dependence of storage modulus (G') and loss modulus (G") for V-catechol gels at 25 °C: A-B/2,5p-amide-V. (ω = 6.28 rad/s). The LVE is maintained up to ~2 % strain for 2p-amide-V and ~42 % strain for 5p-amide-V, after which G′ decreases, and a crossover with G″ is observed at 14% and 86 % respectively.

Table S1. Degradation studies for some representative polymers

Polymer	Crosslinker	Catechol recovered mass (%)
1p-ester	Fe	48
2p-ester	Fe	47
3p-ester	Fe	47
4p-ester	Fe	45
	V	67
5p-amide	Fe	66
	V	32

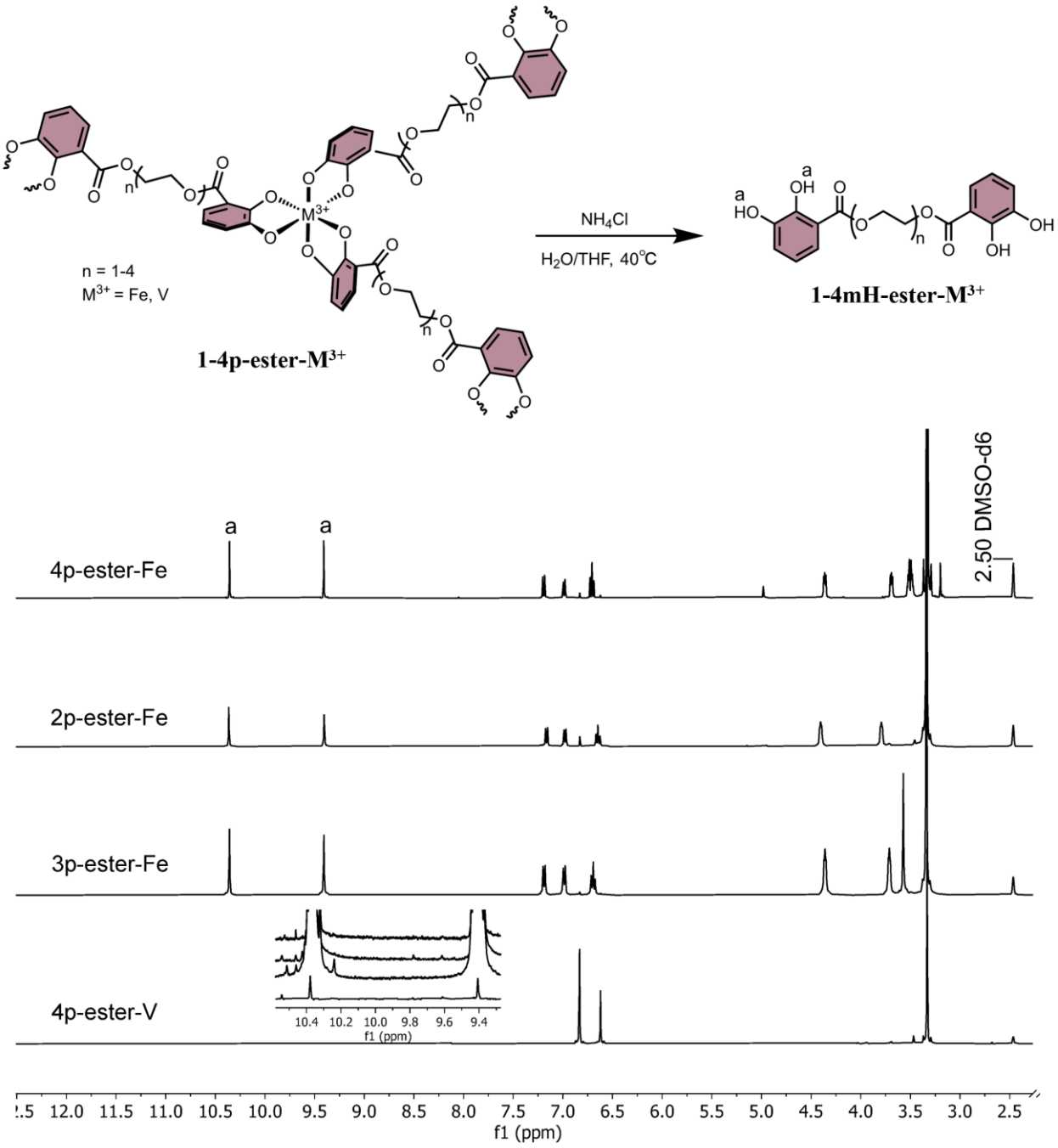

Figure S32. Degradation reaction and ^{1}H NMR spectra of representative esters 2-4p-ester-M^{3+}.

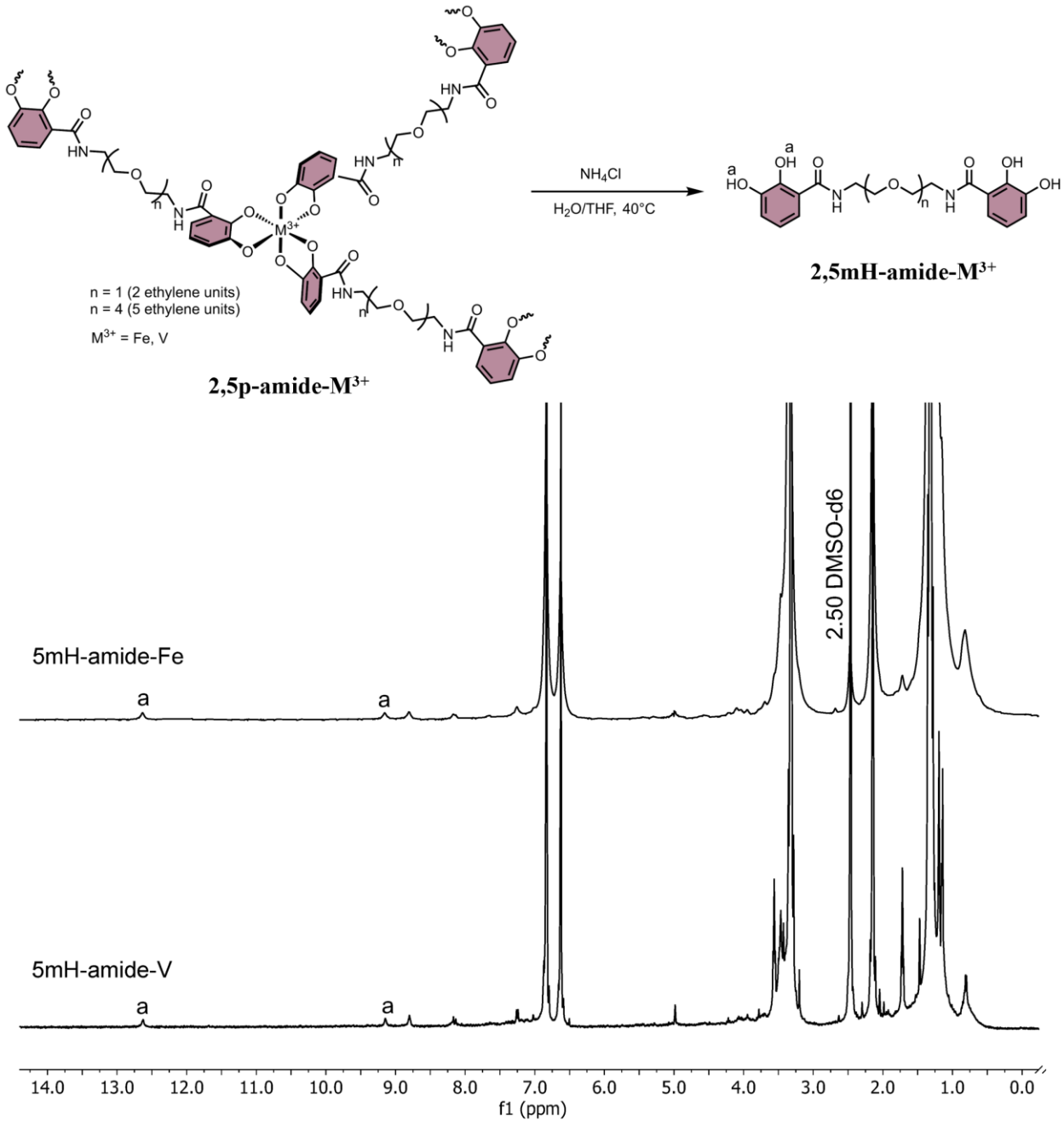

Figure S33 Degradation reaction and ^{1}H NMR spectra of 5p-amide-M^{3+}.